

## Supplementary information

### Ultrafast flash joule heating synthesis of the Pt/MoO<sub>x</sub> heterostructure for enhancing the electrocatalytic hydrogen evolution reaction

Lijuan Zhu,<sup>a</sup> Zhongjie Lai,<sup>a</sup> Jilong Xu,<sup>a</sup> Peiyu Ma,<sup>a</sup> Jiaxiang Lu,<sup>a</sup> Qian Xu,<sup>a</sup> Yitao Lin,<sup>b</sup> Lei Zheng,<sup>c</sup> Lihui Wu,<sup>a</sup> Honghe Ding,<sup>\*a</sup> Jiawei Ge,<sup>\*d</sup> and Yifan Ye<sup>\*a</sup>

<sup>a</sup> National Synchrotron Radiation Laboratory, University of Science and Technology of China, Hefei 230029, PR China.

<sup>b</sup> Department of Engineering Physics, Tsinghua University, Beijing 100084, PR China

<sup>c</sup> Institute of High Energy Physics Chinese Academy of Sciences, Beijing 100049, PR China.

<sup>d</sup> School of Chemistry and Materials Science, University of Science & Technology of China, Anhui 230026, China.

\*Corresponding authors.

*Correspondence authors E-mail address:*

[hhd2016@ustc.edu.cn](mailto:hhd2016@ustc.edu.cn) (Honghe Ding);  
[gejiawei@ustc.edu.cn](mailto:gejiawei@ustc.edu.cn) (Jiawei Ge);  
[yifanye92@ustc.edu.cn](mailto:yifanye92@ustc.edu.cn) (Yifan Ye);

## Supplementary Figures and Tables

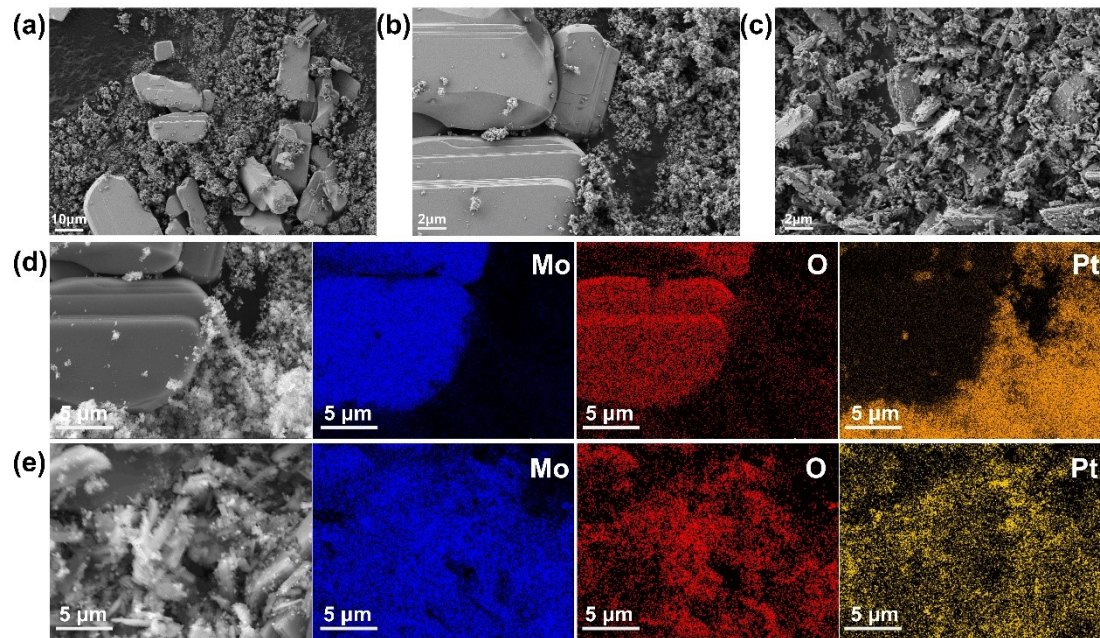


**Fig. S1** SEM images of ungrounded Pt-MoO<sub>3</sub> mixture at 10  $\mu\text{m}$  scale (a) and at 2  $\mu\text{m}$  scale (b). SEM image of grounded Pt-MoO<sub>3</sub> mixture at 2  $\mu\text{m}$  scale (c). The elemental mapping images of ungrounded (d) and grounded (e) Pt-MoO<sub>3</sub> mixture.

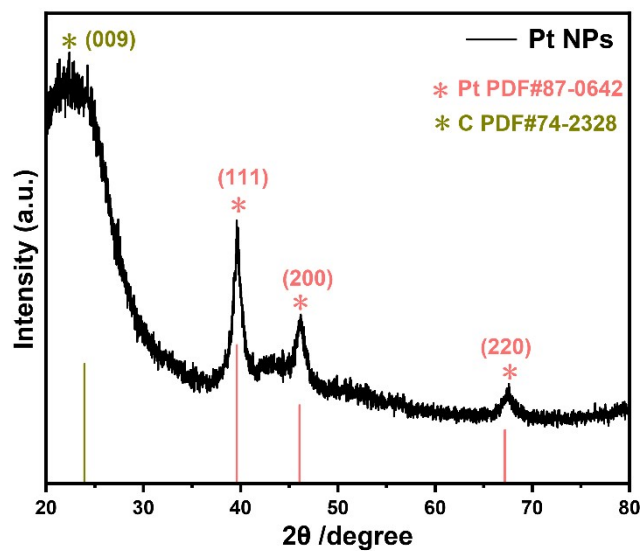


**Fig. S2** The XRD pattern of the Pt NPs.

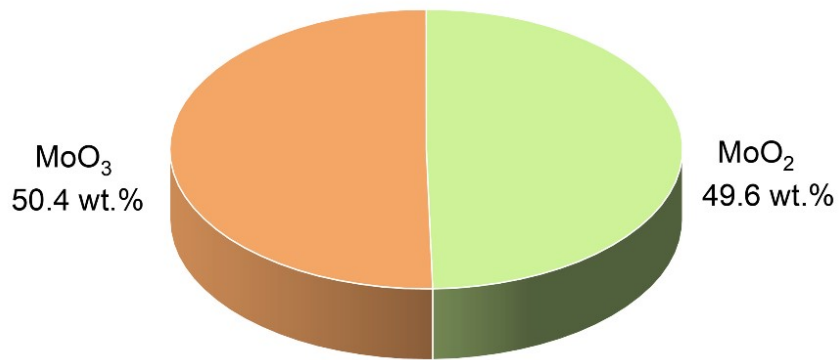


**Fig. S3** The mass ratio of  $\text{MoO}_2$  and  $\text{MoO}_3$  from the quantitative analysis of the XRD of Pt/ $\text{MoO}_x$ -F.

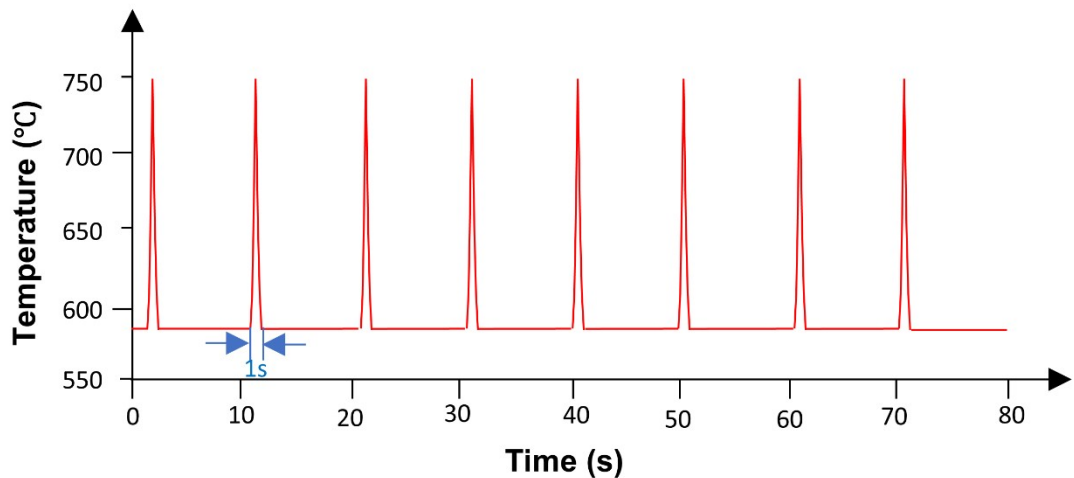


**Fig. S4** Schematic diagram of the temperature-time evolution of the ultrafast joule heating method.

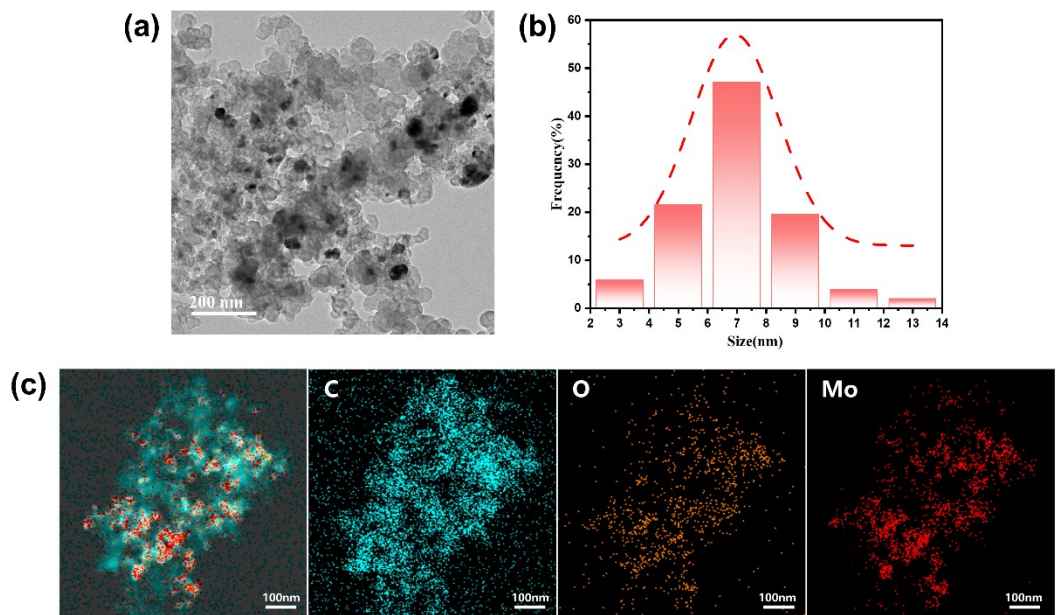


**Fig. S5** (a) The TEM image of  $\text{MoO}_x$ . (b) The size distribution diagram of the metal nanoparticles on the Pt/ $\text{MoO}_x$ -F. (c) The elemental mapping images of  $\text{MoO}_x$ .

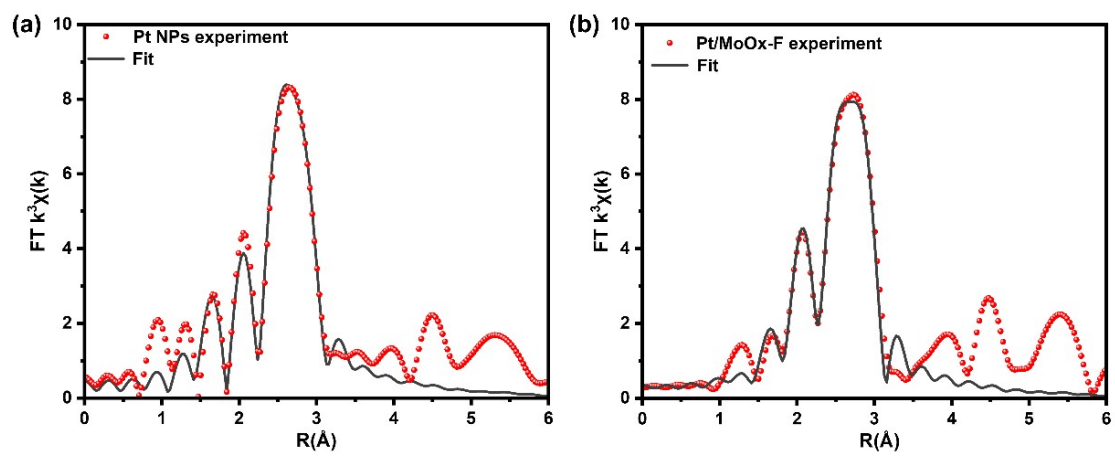


**Fig. S6** Experimental and fitted EXAFS spectra of (a) Pt NPs and (b) Pt/ $\text{MoO}_x$ -F.

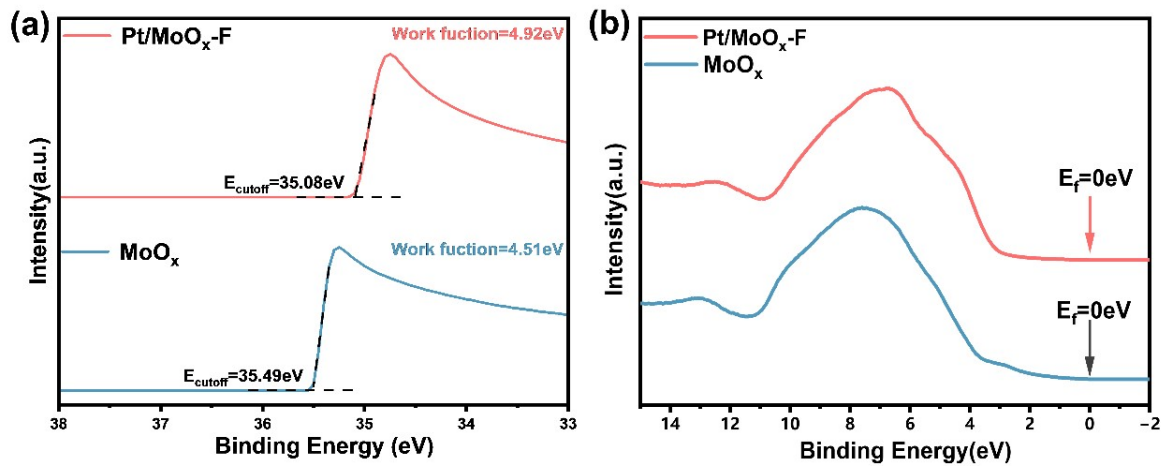


**Fig. S7** UPS spectra of (a) SEC and (b) VB of MoO<sub>x</sub> and Pt/MoO<sub>x</sub>-F samples.

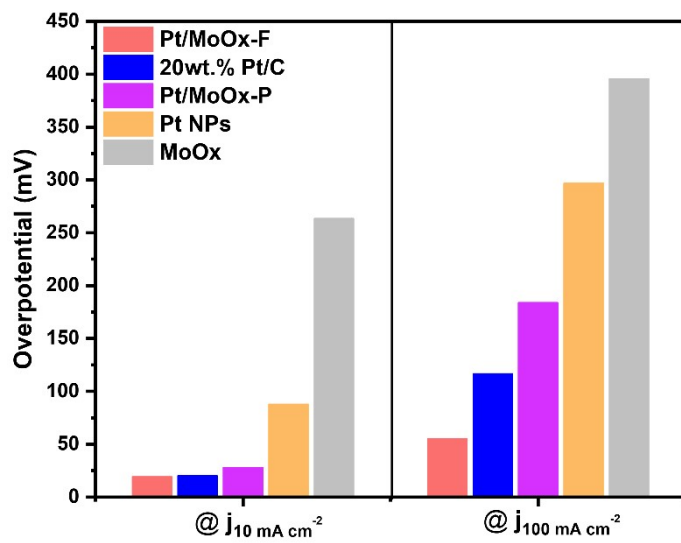


**Fig. S8** The overpotential comparison of Pt/MoO<sub>x</sub>-F and other reference samples at the current density of  $10 \text{ mA cm}^{-2}$  and  $100 \text{ mA cm}^{-2}$ .

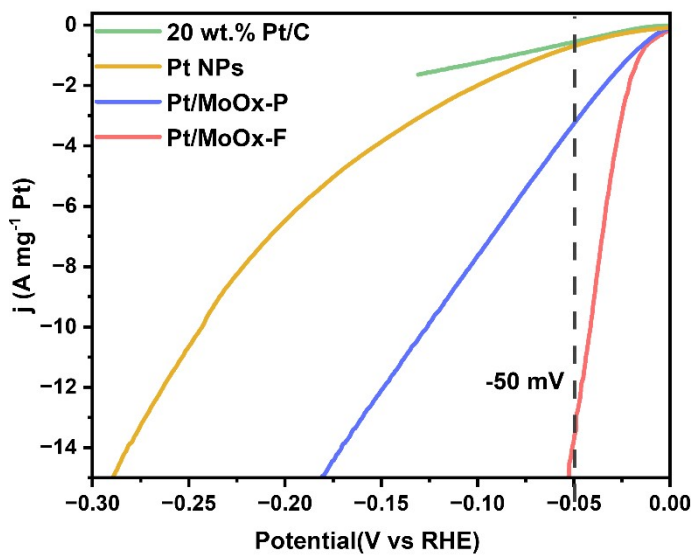


**Fig. S9** LSV curves of as-prepared samples normalized by mass loading of Pt species.

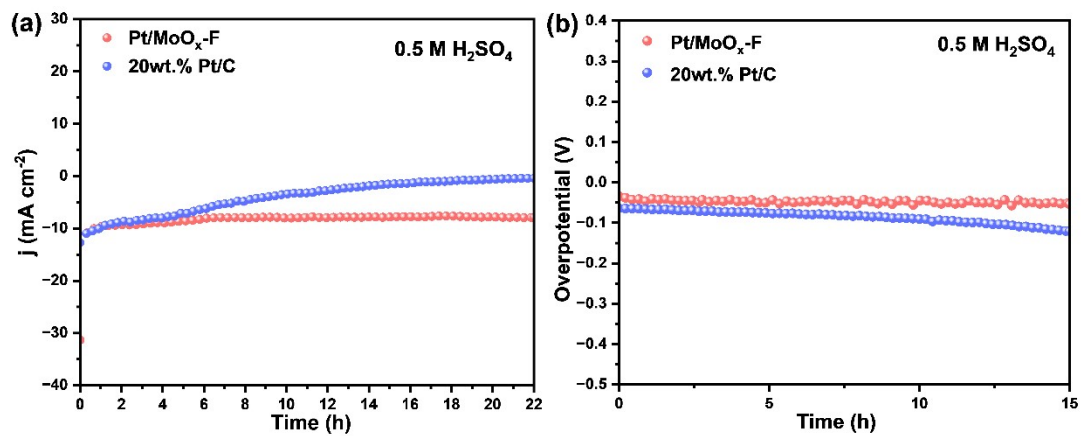


**Fig. S10** (a) The plot of current density versus time for Pt/MoO<sub>x</sub>-F under a constant voltage test in 0.5M H<sub>2</sub>SO<sub>4</sub> electrolyte. (b) The plot of overpotential versus time for Pt/MoO<sub>x</sub>-F under a constant current test.

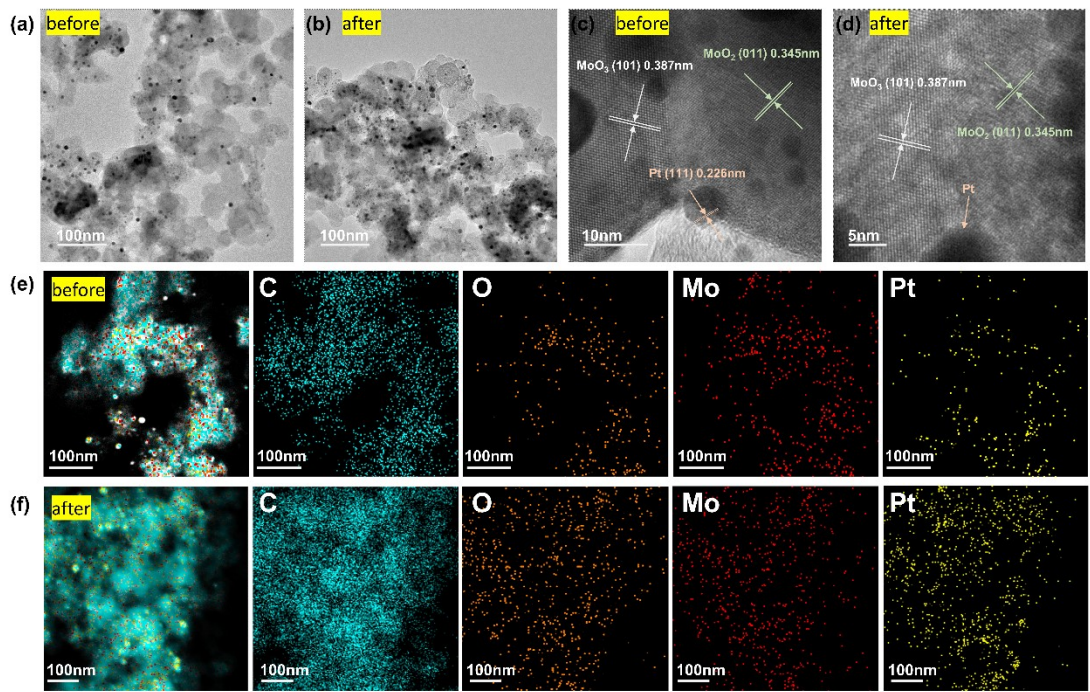


**Fig. S11** Structural changes in the Pt/MoO<sub>x</sub>-F before and after the HER. TEM images of Pt/MoO<sub>x</sub>-F before (a) and after (b) the electrochemical stability tests. HR-TEM images of Pt/MoO<sub>x</sub>-F before (c) and after (d) the electrochemical stability tests. The element distribution images of Pt/MoO<sub>x</sub>-F before (e) and after (f) the electrochemical stability tests.

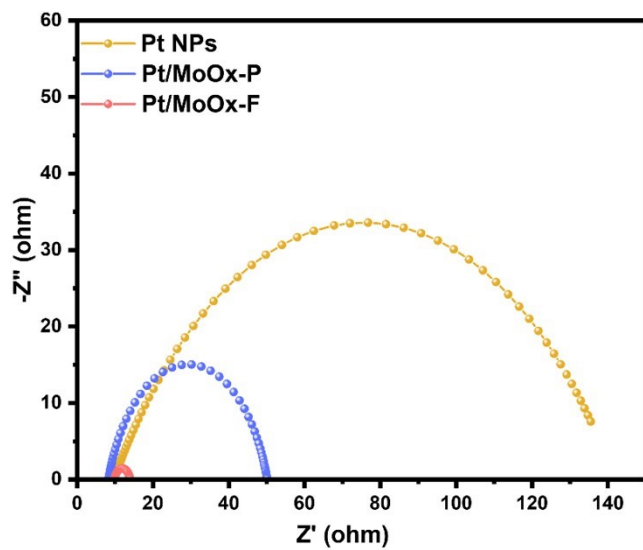


**Fig. S12** Nyquist plots of Pt-MoO<sub>x</sub>-F and reference samples.

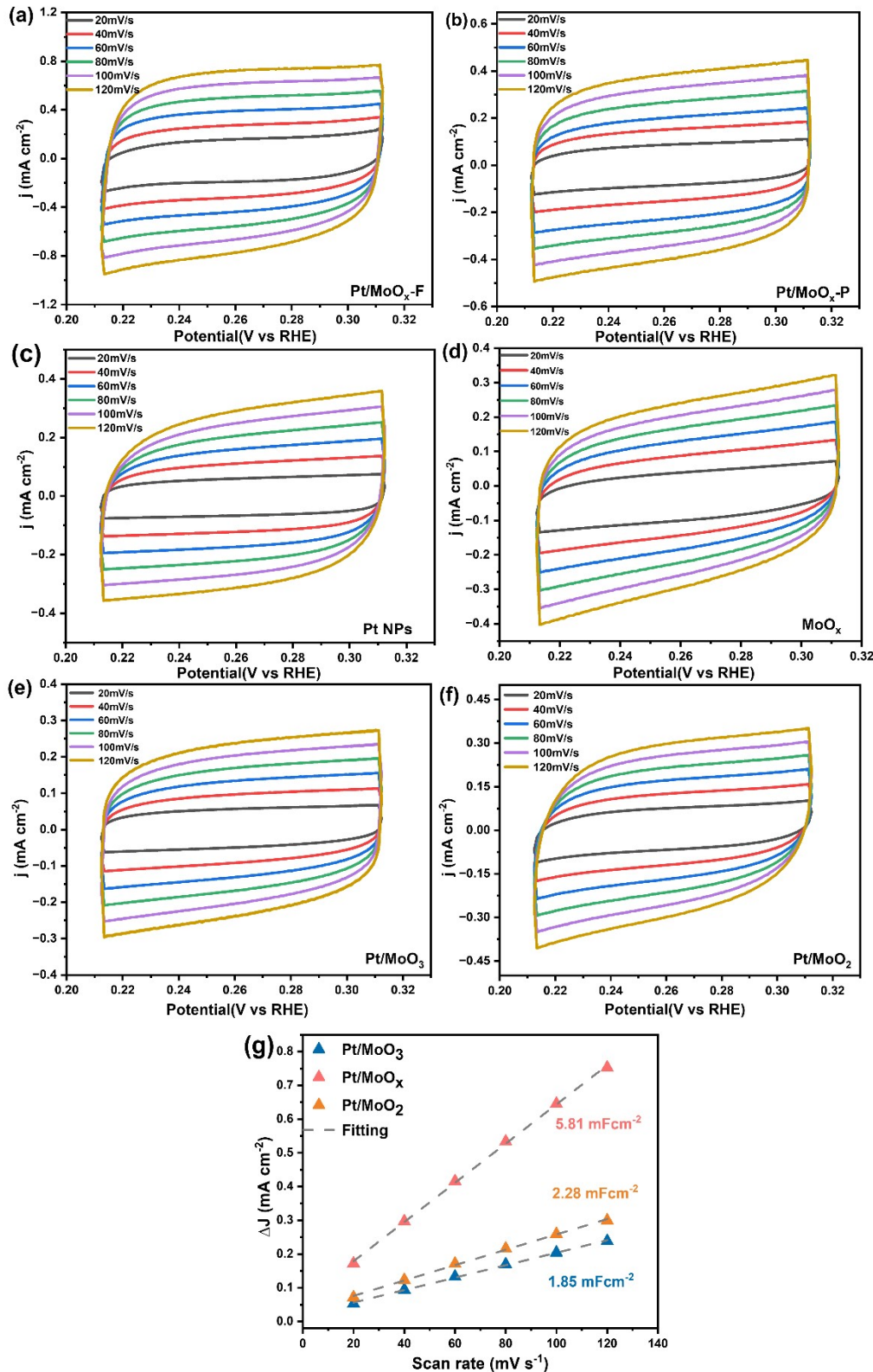


**Fig. S13** Current difference at different scan rates for the estimation of the double-layered capacitance of (a) Pt/MoO<sub>x</sub>-F, (b) Pt/MoO<sub>x</sub>-P, (c) Pt NPs, (d) MoO<sub>x</sub>, (e) Pt/MoO<sub>3</sub> and (f) Pt/MoO<sub>2</sub> in 0.5 M H<sub>2</sub>SO<sub>4</sub>. (g) Capacitive currents as a function of the scan rate of Pt/MoO<sub>2</sub> and Pt/MoO<sub>3</sub> samples.

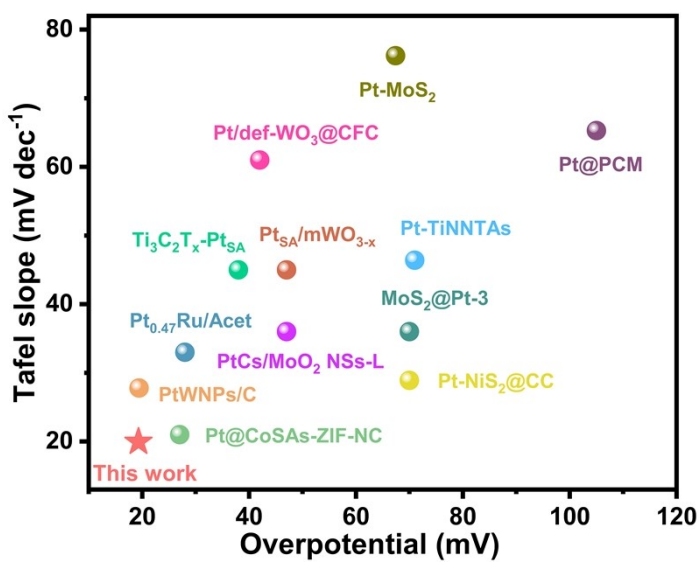


**Fig. S14** In 0.5 M H<sub>2</sub>SO<sub>4</sub> solution, comparison of the overpotentials and Tafel slopes at 10mA cm<sup>-2</sup> with the references.

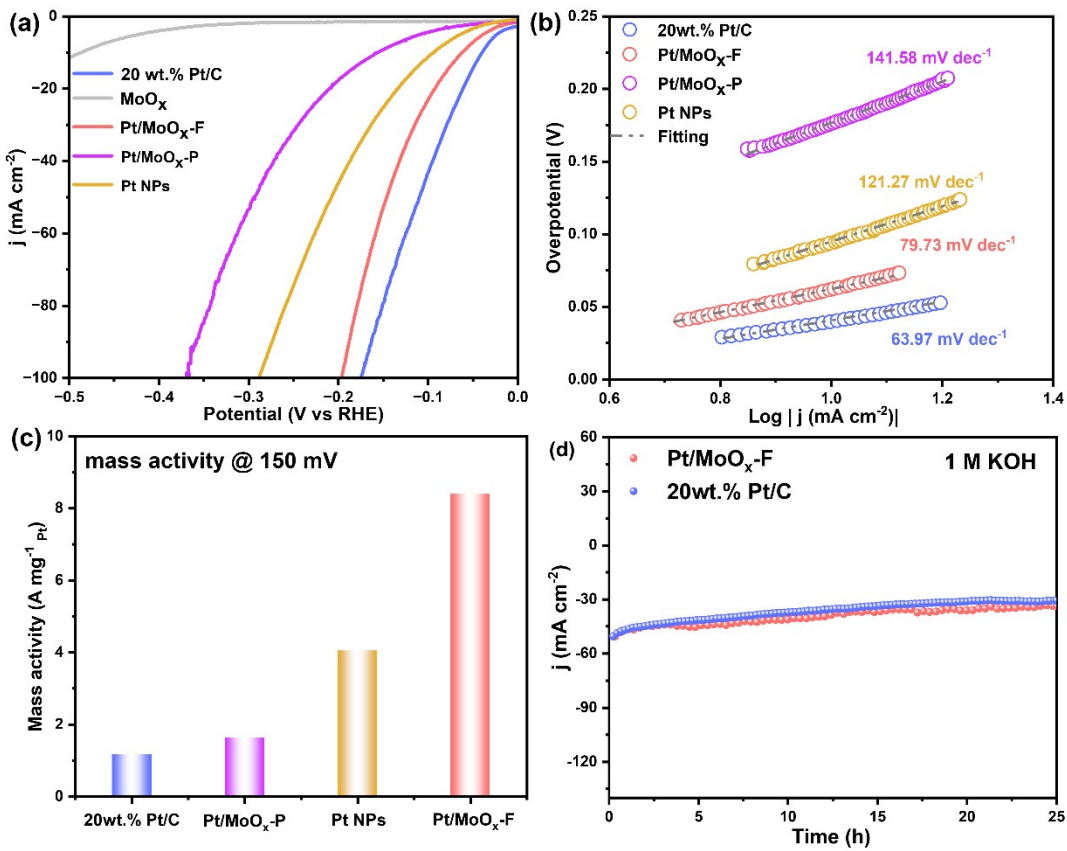


**Fig. S15** Electrochemical HER performance under alkaline electrolyte. (a) Polarization curves of Pt/ $\text{MoO}_x$ -F in comparison with 20 wt.% Pt/C and other reference samples in KOH. (b) Tafel plots for Pt/ $\text{MoO}_x$ -F and other reference samples. (c) Mass activity at  $\eta = 150 \text{ mV}$  of the as-prepared samples. (d) The plot of current density versus time for Pt/ $\text{MoO}_x$ -F under a constant voltage test.

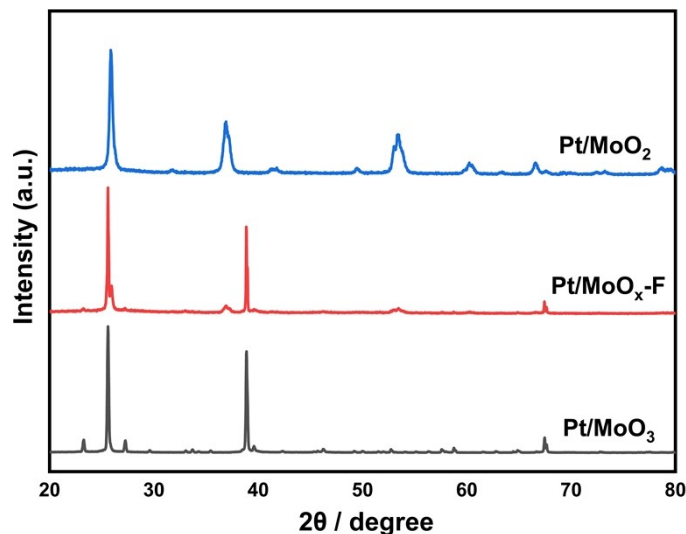


**Fig. S16** XRD patterns of Pt/ $\text{MoO}_x$ -F, Pt/ $\text{MoO}_2$  and Pt/ $\text{MoO}_3$  samples.

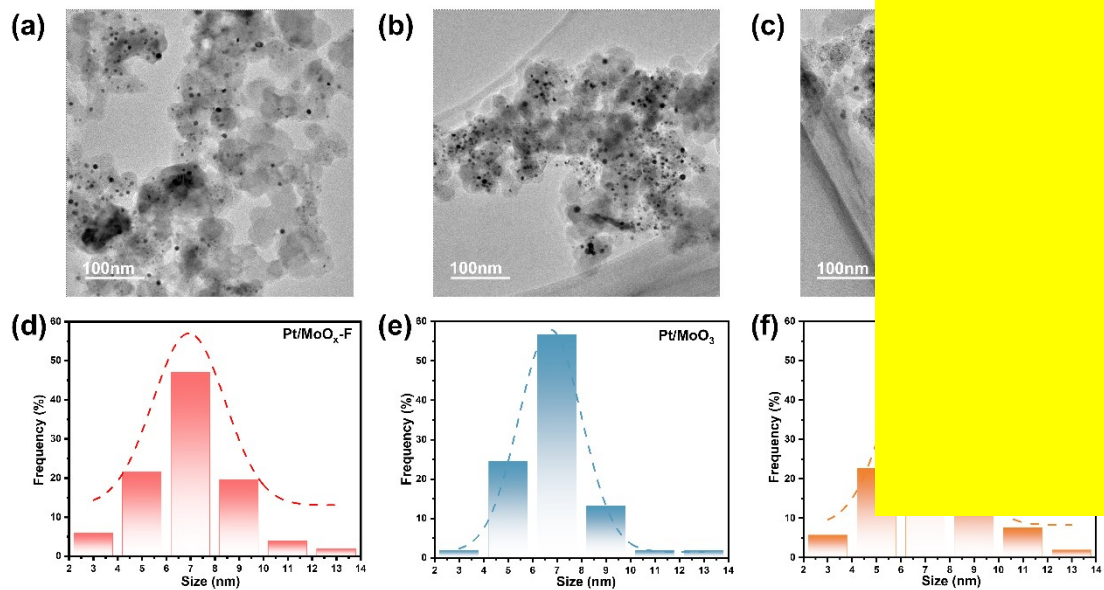


**Fig. S17** (a) TEM image of Pt/MoO<sub>x</sub>-F. (b) TEM image of Pt/MoO<sub>3</sub>. (b) TEM image of Pt/MoO<sub>2</sub>. The size distribution diagram of the metal nanoparticles on the Pt/MoO<sub>x</sub>-F (d), Pt/MoO<sub>3</sub> (e), and Pt/MoO<sub>2</sub> (f).

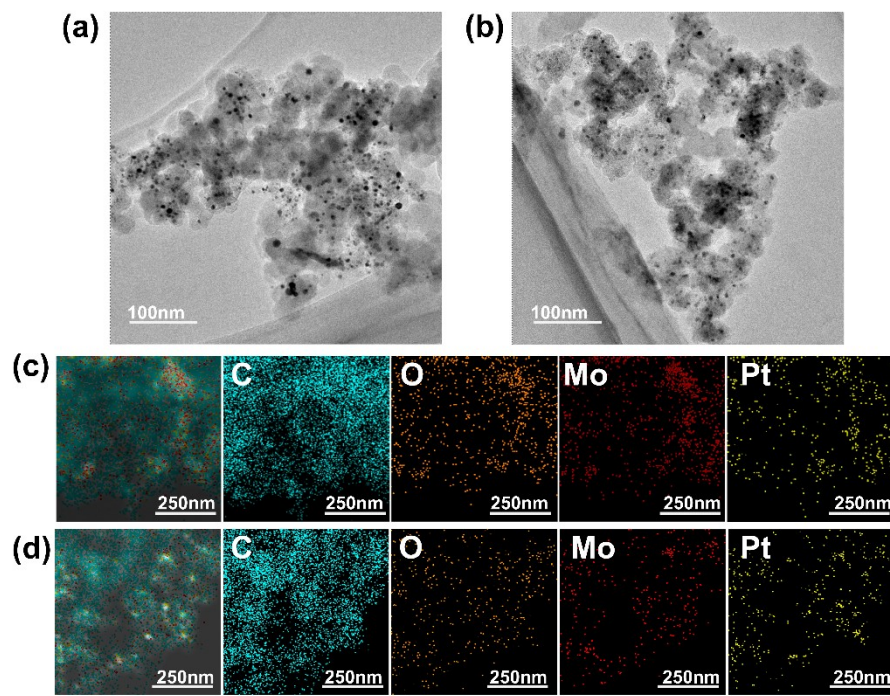


**Fig. S18** (a) TEM image of Pt/MoO<sub>3</sub>. (b) TEM image of Pt/MoO<sub>2</sub>. (c) The elemental mapping images of Pt/MoO<sub>3</sub>. (d) The elemental mapping images of Pt/MoO<sub>2</sub>.

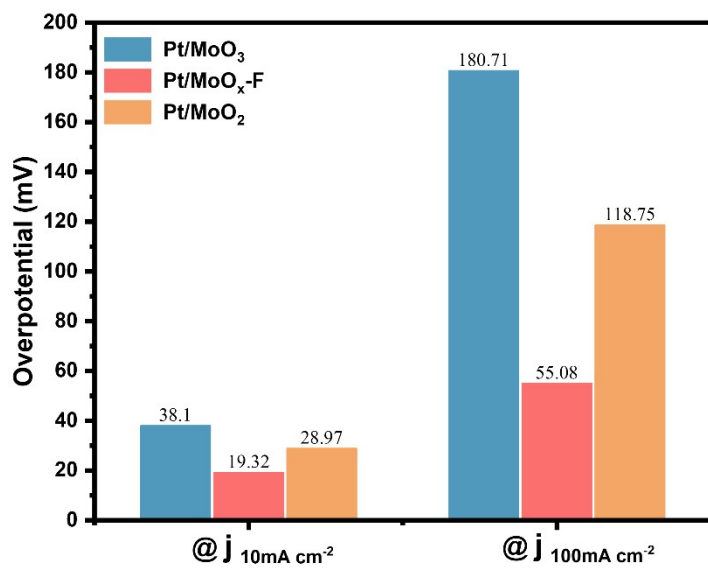


**Fig. S19** The overpotential comparison of Pt/MoO<sub>x</sub>-F and other reference samples at the current density of 10 mA cm<sup>-2</sup> and 100 mA cm<sup>-2</sup>.

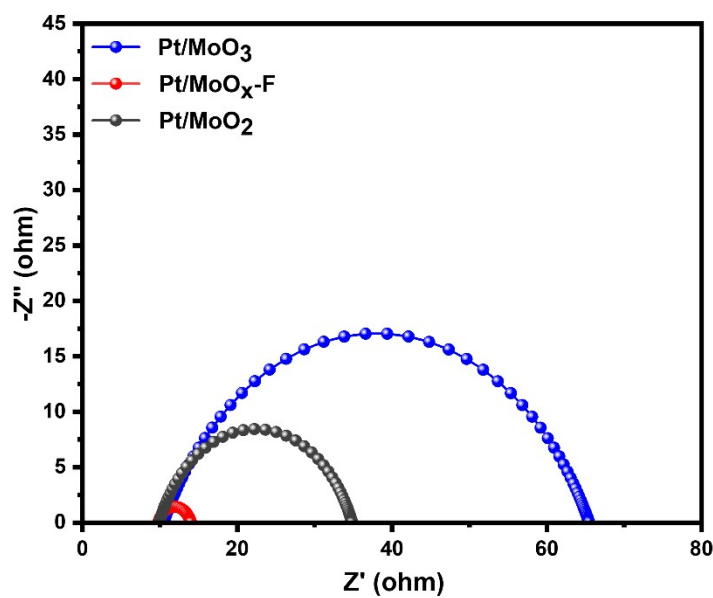


**Fig. S20** Nyquist plots of Pt-MoO<sub>x</sub>-F and reference samples.

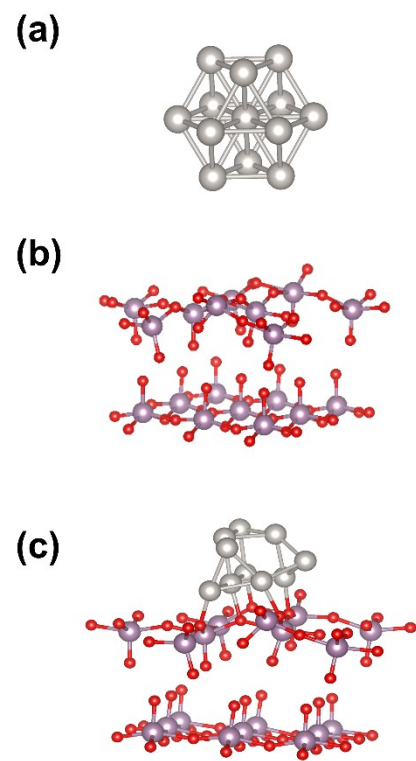


**Fig. S21** The DFT computational models of (a) Pt, (b) MoO<sub>x</sub>-F and (c) Pt/MoO<sub>x</sub>-F.

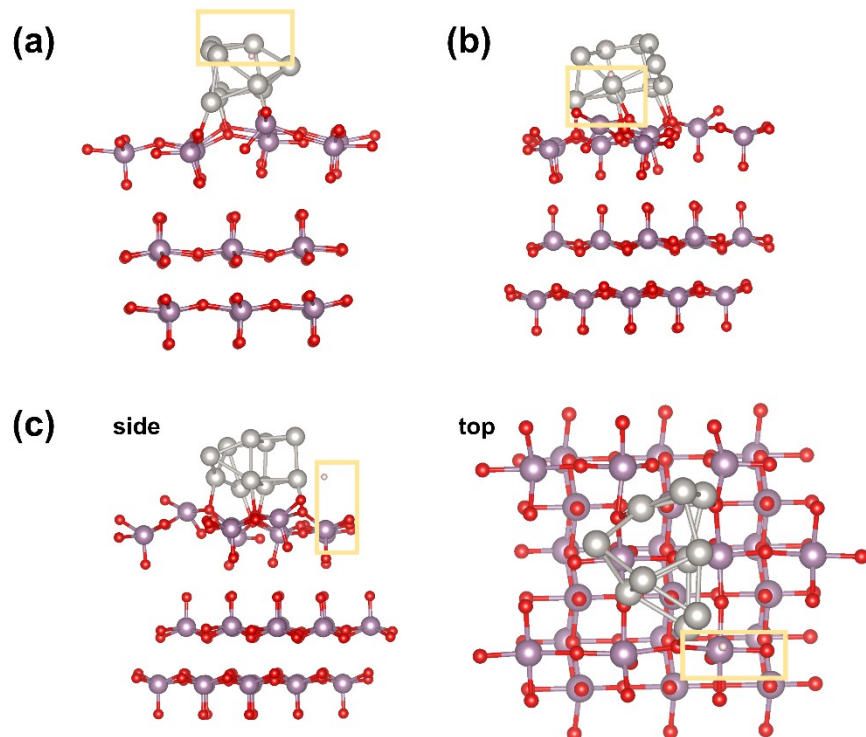


**Fig. S22** The DFT model diagram of three different adsorption hydrogen sites on the Pt/MoO<sub>x</sub>-F.

**Table S1** The spectrogram of the total number of distribution maps of Pt/MoO<sub>x</sub>-F.

Spectrogram of the total number of distribution maps	
Element	Atom %
O	3.76
Mo	1.57

**Table S2** The percentage of Pt loading of as-prepared samples was measured by ICP-AES.

Sample	Pt Content (wt.%)
Pt/MoO <sub>x</sub> -F	1.853
Pt/MoO <sub>x</sub> -P	1.854
Pt NPs	1.857
Pt/MoO <sub>3</sub>	1.853
Pt/MoO <sub>2</sub>	1.856

**Table S3** The EXAFS fitting results of Pt/MoO<sub>x</sub>-F and reference samples.

sample	path	CN	Bond length(Å)	Debye-Walker coefficient (Å <sup>2</sup> )	△E <sub>0</sub> (eV)	R factor
Pt foil	Pt-Pt	12	2.76	0.004	7.97	0.001
PtO <sub>2</sub>	Pt-O	6	2.00	0.003	9.37	0.009
Pt NPs	Pt-Pt	6.18	2.76	0.005	8.23	0.008
	Pt-O	1.12	2.00	0.007		
Pt/MoO <sub>x</sub> -F	Pt-Pt	8.67	2.76	0.006	7.74	0.016
	Pt-O	0.51	2.01	0.009		
	Pt-Mo	0.94	2.75	0.008		

Binding Energies (eV)								
Samples	Mo <sup>4+</sup>		Mo <sup>5+</sup>		Mo <sup>6+</sup>		Pt	
	Mo3d <sub>5/2</sub>	Mo3d <sub>3/2</sub>	Mo3d <sub>5/2</sub>	Mo3d <sub>3/2</sub>	Mo3d <sub>5/2</sub>	Mo3d <sub>3/2</sub>	Pt4f <sub>7/2</sub>	Pt4f <sub>5/2</sub>
MoO <sub>x</sub>	229.25	232.38	231.41	234.54	232.71	235.84	-	-
Pt/MoO <sub>x</sub> -F	-	-	231.63	234.76	232.65	235.78	71.65	74.95
Pt NPs	-	-	-	-	-	-	72.23	75.53

**Table S4** The XPS spectra-specific parameters.

**Table S5.** Comparison of HER performance between Pt/MoO<sub>x</sub>-F and the recently reported Pt-based electrocatalysts in 0.5 M H<sub>2</sub>SO<sub>4</sub>.

Sample	$\eta_{10}$ (mV)	$\eta_{100}$ (mV)	Mass activity (A mg <sup>-1</sup> Pt)	Tafel slope (mV dec <sup>-1</sup> )	Reference
Pt/MoO <sub>x</sub> -F	19.32	55.08	13.80@50mV	19.94	This work
Pt-SAs/WS <sub>2</sub>	32	170	130.2@100mV	28	[1]
Mo <sub>2</sub> TiC <sub>2</sub> T <sub>x</sub> Pt <sub>S</sub> A	30	77	8.3@77 mV	30	[2]
Pt <sub>SA</sub> /mWO <sub>3-x</sub>	47	-	12.8@50 mV	45	[3]
Pt-TiO <sub>2-x</sub> NSs	36	180	~0.85@150mV	32.1	[4]
Pt <sub>0.47</sub> Ru/Acet	28	~80	2.63@100mV	33.3	[5]
Pt/Ni-DA	18	-	2.13@50mV	34	[6]
Pt-WO <sub>x</sub> /WS <sub>2</sub>	42	~300	0.68@112 mV	26	[7]
Pt-MoS <sub>2</sub>	67.4	-	-	76.2	[8]
Pt <sub>SA</sub> /NT/NF	30	88	0.93@100mV	-	[9]
Pt/V <sub>2</sub> O <sub>3</sub> /V <sub>8</sub> C <sub>7</sub>	45	78	0.64@100mV	30.2	[10]
Pd7@Pt3	33	90	-	23.1	[11]
0.8% Pt-Naf- CV	34	143	-	33	[12]
PtW NPs/C	19.4	-	0.566@20mV	27.8	[13]
Pt <sub>SA</sub> / $\alpha$ - MoC <sub>1-x</sub> @C- 0.75	12	120	31.56@100mV	27	[14]

## References:

- [1] Y. Shi, Z. Ma, Y. Xiao, Y. Yin, W. Huang, Z. Huang, Y. Zheng, F. Mu, R. Huang, G. Shi, Y. Sun, X. Xia and W. Chen, *Nat. Commun.*, 2021, **12**, 3021.
- [2] J. Zhang, Y. Zhao, C. Chen, C. Dong, R. Liu, C. Han, Y. Li, Y. Gogotsi and G. Wang, *Nat. Catal.*, 2018, **1**, 985-992.
- [3] J. Park, S. Lee, H. E. Kim, A. Cho, S. Kim, Y. Ye, J. W. Han, H. Lee, J. H. Jiang and J. Lee, *Angew. Chem., Int. Ed.*, 2019, **131**, 16184.
- [4] K. M. Naik, *Nanoscale*, 2020, **12**, 11055-11062.
- [5] Y. Chen, J. Li, N. Wang, Y. Zhou, J. Zheng and W. Chu, *Chem. Eng. J.*, 2022, **448**, 137611.
- [6] Y. Peng, K. Ma, T. Xie, J. Du, L. Zheng, F. Zhang, X. Fan, W. Peng, J. Ji and Y. Li, *ACS Appl. Mater.*, 2023, **15**, 27089–27098.
- [7] L. S. Oh, J. Y. Kim, H. W. Kim, J. Han, E. Lim, W. B. Kim, J. H. Park and H. J. Kim, *Chem. Commun.*, 2021, **57**, 11165-11168.
- [8] A. Shan, X. Teng, Y. Zhang, P. Zhang, Y. Xu, C. Liu, H. Li, H. Ye and R. Wang, *Nano Energy*, 2022, **94**, 106913.
- [9] L. Zhang, L. Han, H. Liu, X. Liu and J. Luo, *Angew. Chem. Int. Ed.*, 2017, **56**, 13694-13698.
- [10] Y. Li, Y. Sheng, L. Shao, Y. Li, W. Xu, S. Zhang, F. Shao and J. Wang, *J. Mater. Chem. A*, 2024, **12**, 8724-8733.
- [11] Y. Liu, N. Yodsin, T. Li, H. Wu, R. Jia, L. Shi, Z. Lai, S. Namuangruk and L. Huang, *Mater. Horiz.*, 2024, **11**, 1964-1974.
- [12] J. Yu, D. Wei, Z. Zheng, W. Yu, H. Shen, Y. Qu, S. Wen, Y. U. Kwon and Y. Zhao, *J. Colloid Interface Sci.*, 2020, **566**, 505-512.
- [13] D. Kobayashi, H. Kobayashi, D. Wu, S. Okazoe, K. Kusada, T. Yamamoto, T. Toriyama, S. Matsumura, S. Kawaguchi, Y. Kubota, S. M. Aspera, H. Nakanishi, S. Arai and H. Kitagawa, *J. Am. Chem. Soc.*, 2020, **142**, 17250-17254.
- [14] W. Wang, Y. Wu, Y. Lin, J. Yao, X. Wu, C. Wu, X. Zuo, Q. Yang, B. Ge, L. Yang, G. Li, S. Chou, W. Li and Y. Jiang, *Adv. Funct. Mater.*, 2022, **32**, 2108464.